HHS Public Access

Author manuscript

Biomaterials. Author manuscript; available in PMC 2020 December 01.

Published in final edited form as:

Biomaterials. 2019 December ; 223: 119476. doi:10.1016/j.biomaterials.2019.119476.

A Long Acting Nanoformulated Lamivudine ProTide

Nathan Smith[a], **Aditya N. Bade**[a], **Dhruvkumar Soni**[b], **Nagsen Gautam**[b], **Yazen Alnouti**[b], **Jonathan Herskovitz**[a], **Ibrahim M. Ibrahim**[a], **Melinda S. Wojtkiewicz**[a], **Bhagya Laxmi Dyavar Shetty**[a], **JoEllyn McMillan**[a], **Howard E. Gendelman**[a,b,*,‡], **Benson Edagwa**[a,*]

[a]Department of Pharmacology and Experimental Neuroscience, University of Nebraska Medical Center, Omaha, NE 68198 USA

[b]Department of Pharmaceutical Sciences, University of Nebraska Medical Center, Omaha, NE 68198 USA

Abstract

A long acting (LA) hydrophobic and lipophilic lamivudine (3TC) was created as a phosphoramidate pronucleotide (designated M23TC). M23TC improved intracellular delivery of active triphosphate metabolites and enhanced antiretroviral and pharmacokinetic (PK) profiles over the native drug. A single treatment of human monocyte derived macrophages (MDM) with nanoformulated M23TC (NM23TC) improved drug uptake, retention, intracellular 3TC triphosphates and antiretroviral activities in MDM and CD4+ T cells. PK tests of NM23TC administered to Sprague Dawley rats demonstrated sustained prodrug and drug triphosphate levels in blood and tissues for 30 days. The development of NM23TC remains a substantive step forward in producing LA slow effective release antiretrovirals for future clinical translation.

Keywords

Lamivudine; prodrug; ProTide; formulation; long-acting; antiretroviral therapy

[*]**Co-corresponding authors:** Howard E. Gendelman, M.D., Department of Pharmacology and Experimental Neuroscience, University of Nebraska Medical Center, Omaha, NE 68198-5880, USA; phone: 402-559-8920; fax: 402-559-3744; hegendel@unmc.edu and Benson Edagwa, Ph.D., Department of Pharmacology and Experimental Neuroscience, University of Nebraska Medical Center, Omaha, NE 68198-5800, USA; phone: 402-559-3093; fax: 402-559-7495; benson.edagwa@unmc.edu. [‡]**Communication author (for submission and review)**: Howard E. Gendelman, M.D., Department of Pharmacology and Experimental Neuroscience, University of Nebraska Medical Center, Omaha, NE 68198-5880, USA; phone: 402-559-8920; fax: 402-559-3744; hegendel@unmc.edu.

Author contributions

B.E. – conceived project, study design, design of synthesis and formulation experiments, supervision of experiments, data analysis and interpretation; H.E.G. – conceived project, designed the experiments and data interpretations. N.S. – study design, design and execution of experiments, data acquisition, data analysis and interpretation; D.S. – synthesis of prodrug. J.M., A.B. and N.S. co-designed the animal studies. A.B. and N.S. performed the PK experiments in mice. A.B. designed and performed toxicity assays in rats. Y.H. assisted in design and execution of T cell work. I.M.I. assisted in cell isolation in PK studies. N.G., B.S. M.W., and J.M. developed, performed and analyzed the UPLC/MS/MS analyses and in vivo blood and tissue quantitation. N.G., Y.A., and N.S. designed protocols and analyzed 3TC-TP data. H.E.G., B.E., and N.S. wrote the manuscript.

Supplementary Material (See attached document)

Conflict of Interest: Declarations of interest: none

Data Availability: The raw/processed data required to reproduce these findings cannot be shared at this time due to technical or time limitations.

The authors have no affiliations or financial involvement with any organization or entity with a financial interest in or financial conflict with the subject matter or materials discussed in the manuscript apart from those disclosed. We would like to acknowledge Dr. Kamel Khalili for providing NL4–3 eGFP pseudovirus used in these studies.

1. Introduction

Antiretroviral therapy (ART) has revolutionized human immunodeficiency virus type one (HIV-1) care and prevention by changing disease outcomes from certain death to viable high quality life [1]. Despite such successes notable needs still remain. These include the stigma of daily use drug requirements and breaks in regimen adherence from treatment fatigue [2]. These, in turn, speed viral drug resistance and adverse events. With these needs in mind optimized HIV-1 treatment and prevention strategies were sought and long acting (LA) antiretroviral drugs (ARVs) were created [3, 4]. Despite early efforts, broad use of the few available LA drug formulations is limited, dictated by inherent physicochemical properties of the parent compounds, the mandated frequency of injections and the administered dosing volumes [5]. Thus, and through innovative medicinal and polymer chemistry the field of long acting slow effective release ART (LASER ART) was birthed, defined as potent physicochemical stable hydrophobic and lipophilic ARVs with simple scale ups [6–8].

As of today, two nucleoside reverse transcriptase inhibitors (NRTIs), tenofovir (TDF), lamivudine (3TC) and/or emtricitabine (FTC), taken with the integrase inhibitor dolutegravir are current “first line” combination ART [9, 10]. Whereas administration is offered in a single pill the drugs’ relatively short half-lives require daily life-long administration [9]. Due, in measure, to long-term human immunodeficiency virus (HIV) infection, limited lymphoid and brain drug tissue penetrance, inherent drug toxicities and malabsorption syndromes, opportunities for further regimen improvement(s) abound [10]. These provide opportunities for new LASER ART product developments [6, 8, 11, 12]. Defined by the transformation of partially hydrophobic and hydrophilic ARVs into water insoluble lipophilic prodrug nanocrystals [6–8, 11, 13, 14], LASER ART serves to improve ARV pharmacokinetic (PK) and pharmacodynamic (PD) profiles [7, 8]. The translational potential is based on maintenance of therapeutic drug concentrations at restricted sites of infection and formulation stability over a broad range of temperature and pH [15]. Thus, advancing evidence demonstrates that LASER ART could occupy a seat in next stage developments of LA ART injectables [6].

While allowing ease of scale up and long-term prodrug and particle stability in first generation LASER ART, therapeutic success would require modifications to extend drug half-life from weeks to months. Moreover, slow prodrug hydrolysis rates along with ARV entry into “putative” viral reservoirs will be required [6]. Based on what is now an extensive body of work, second generation LASER ART formulations are being developed [7, 8, 13, 14, 16]. Prior modifications of the primary hydroxyl or amine groups in 3TC generated hydrophobic ester or carbamate prodrug derivatives with limited intracellular drug levels. In the current report 3TC was transformed into a sustained release potent medicine. We deployed a ProTide technology based on successful prior works where “like” conversions were made of sofosbuvir and tenofovir alafenamide (TAF) [17–19]. However, the current goal was to produce an injectable hydrophobic and lipophilic prodrug. We provide support for the fact that physicochemical transformation leads to alterations in the prodrug’s solubility in water and lipids with improved drug potency and membrane permeability [11, 20]. To achieve these desired physicochemical properties a structure-based screening of a range of amino acid and phosphonate ester promoieties was implemented. These culminated

in the identification of a lipophilic sustained release poloxamer-coated and potent ARV nanosuspension as previously reported for abacavir (ABC) [16]. While the concept of ProTide technology is decades old [18, 21], its prior application focused on affecting drug potency and safety not in producing LA formulations [22]. Indeed, current LA ARVs, cabotegravir (CAB) or rilpivirine (RPV), now advanced to phase III clinical trials [23, 24] are hydrophobic, facilitating their immediate use as injectables [25]. In contrast, tenofovir alafenamide and sofusbuvir possess high aqueous solubility [26, 27] with poor conversion to LA nanosuspensions. Thus, transformation of 3TC into a lipophilic ProTide nanocrystal is unique as it serves to facilitate prolonged intracellular accumulation of 3TC triphosphate and improve its biodistribution and potency. Our goal was to create controlled and sustained intracellular 3TC delivery by maintaining intracellular concentrations of its active metabolite within the therapeutic range.

2. Materials and Methods

2.1. Chemical Reagents

3TC was purchased from Boc Sciences (Shirley, NY). Phenyl dichlorophosphate, N-(carbobenzyloxy)- L-phenylalanine, docosanol, dichloromethane (CH_2Cl_2), chloroform ($CHCl_3$), *N,N*-dimethylformamide (DMF), $(CD_3)_2SO$, triethylamine (Et_3N), diethyl ether, tetrahydrofuran (THF), tert-butylmagnesium chloride solution (^{t}BuMgCl, 1.0M in THF), triethylsilane (Et_3SiH), pluronic F127 (P407), and 1-octanol, were purchased from Sigma-Aldrich (St. Louis, MO). LC-MS grade water and methanol were purchased from Fisher Scientific (Waltham, MA).

Distearoylphosphatidylethanolamine-methyl-polyethylene glycol conjugate-2000 ($mPEG_{2000}$-DSPE) was purchased from Corden Pharma (Cambridge, MA). 1-[Bis(dimethylamino)methylene]-1H-1,2,3-triazolo[4,5-b] pyridinium 3-oxid hexafluoro-phosphate (HATU) was obtained from Chem-Impex International Inc. (Wood Dale, Illinois). Palladium, 10% on activated carbon, was purchased from STREM Inc. (Newburyport, MA). All the chemical reactions were performed under a dry argon atmosphere. Flash chromatography was performed using 32–63 μm flash silica gels from SiliCycle Inc. (Quebec, Canada). Reactions were monitored by thin-layered chromatography on precoated silica plates (250 μm, F-254; SiliCycle Inc.). The compounds were visualized by UV fluorescence. Heat-inactivated pooled human serum was purchased from Innovative Biologics (Herndon, VA). CEM-CD4+ T cells (CEM-SS; cat # 776) were obtained from the National Institutes of Health.

2.2. Prodrug Synthesis

3TC (1.0g, 4.36 mmol, 1 equivalents) was dried azeotropically from anhydrous pyridine (10 mL), resuspended in anhydrous THF (30 mL), cooled to −78°C, followed by addition of ^{t}BuMgCl (5.23 mmol, 1.2 equivalents) and allowed to stir for 15 minutes under an argon atmosphere. A solution of aryl phenylalanyl docosyl ester phosphorochloridate (2.5g, 4.36 mmol, 1 equivalent) was prepared with protocol modifications [16]. The created solution was dissolved in THF (20 mL) followed by dropwise addition to the 3TC anion at −78°C. The reaction mixture was gradually warmed to room temperature and stirred for 48 hours.

M23TC was then isolated by silica gel column flash chromatography purification using a mobile phase of 95:5 DCM:MeOH and lyophilized to form a colorless powder (67% yield). The desired chemical structure was confirmed by nuclear magnetic resonance (NMR) spectroscopy, Fourier Transform Infrared Spectroscopy (FTIR) and by infusion into a triple quadrupole mass spectrometer. Solubilities of 3TC and M23TC were determined by adding excess of each compound to water or 1-octanol. The homogeneous saturated solutions were mixed at room temperature for 24 hours and centrifuged at 17,000 x *g* for 10 minutes to pellet insoluble drug. The amount of drug in the supernatants was quantified by multiple reaction monitoring (MRM) on a liquid chromatography tandem mass spectrometry

To evaluate prodrug stability, 100 μL plasma from different species (rat, human, mouse, and rabbit) was incubated with 1 μM M23TC in non-saturating conditions. Triplicate samples for each species and timepoint were kept in amber glass vials on a shaker at 37°C with slow shaking. At 0 min and 2, 6 and 24 hours after incubation, 900 μL of methanol was added to each vial and vortexed for 3 min to stop the reaction. For 0-min time-point, and to account for non-specific binding, a 100 μL ice cold plasma was spiked with 1 μl of a spiking solution, containing 100 μM prodrug in DMSO, then 900 μl of Ice cold MeOH was immediately added. Upon collection, samples were vortexed for 3 minutes, centrifuged at 16,000 x *g* for 10 minutes, supernatant was aspirated, and evaporated under vacuum. Samples were then reconstituted in 80% methanol (100 μL), centrifuged at 16,000 x *g* for 10 minutes and the supernatant was analyzed by UPLC-MS/MS.

Prodrug and parent drug effects on cell viability were measured in primary MDM and CEM-CD4+ T cells. Human monocytes were isolated [28] then cultured for 7–10 days in 48 well plates (200,000 cells/well) with Dulbecco's Modified Eagles Media (DMEM) supplemented with 10% heat-inactivated pooled human serum, 1,000 U/ml of macrophage colony stimulating factor, 1% glutamine, 10 μg/mL ciprofloxacin, and 50 μg/mL gentamicin in a 37°C 5% CO_2 incubator. A stock solution of each drug in DMSO was serially diluted in DMEM to produce concentrations ranging from 1–200 μM. Cells were treated for 24 hours, washed and incubated with 200 μL/well 3-(4,5-dimethylthiazol-2-yl)-2,5-diphenyltetrazolium bromide (MTT) solution (5 mg/mL) for 45 minutes. Upon MTT removal, 200 μL/well of DMSO was added and absorbance measured at 490 nm on a SpectraMax M3 plate reader with SoftMax Pro 6.2 software (Molecular Devices, San Jose, CA). Sample responses were determined as a percentage of non-treated control response. CEM-CD4+ T cells were added to a U-bottom 96 well plate at 10^5 cells per well in Roswell Park Memorial Institute (RPMI) media with 10% fetal bovine serum, 1% penicillin, and 1% streptomycin and treated with 3TC or M23TC as described for MDM. After 24 hours, cells were centrifuged at 650 x *g*, dispersed in PBS, centrifuged again at 650 x *g*, and resuspended in PBS. Dead cells were counted with Live/Dead Fixable Dead Cell Stain Kit (Life Technologies Corporation. Eugene, Oregon). Briefly, 0.1μL/million cells green fluorescent excitation dye (dissolved in DMSO) was added to each well. Cell were left at room temperature for 30 minutes in the dark. Cells were then centrifuged at 650 x *g*, washed twice in 100 μL PBS with 1% BSA and resuspended in 100μL PBS with 1% BSA. Cells were excited at 488 nm and detected at 530 nm using flow cytometry. Fluorescent cells were gated and counted as % dead. Live cells were then calculated as 100%-%dead. Identical MTT measurements as done in MDM were used as confirmation.

2.2.1. Prodrug and Nanoformulation Characterization— ^{1}H-NMR, ^{13}C-NMR and ^{31}P-NMR spectra were recorded on a Varian Unity/Inova-500 NB (500 MHz; Varian Medical Systems Inc., Palo Alto, CA, USA). FTIR was performed using a Spectrum Two FT-IR spectrometer (Perkin Elmer, Waltham, MA, USA). Infusion into a Waters Xevo TQ-S micro triple quadrupole mass spectrometer (Waters, Milford, MA) was used to confirm a m/z of 841.54. Predicted isotopic distribution was m/z: 840.46 (100.0%), 841.47 (49.7%), 842.47 (13.9%), 842.46 (5.3%), 843.47 (2.8%), 843.46 (2.3%), 841.46 (2.3%). Drug quantitation measurements were performed by LC-MS/MS using a Waters ACQUITY H-class ultra-performance liquid chromatography (UPLC) system (Waters, Milford, MA) coupled to a Waters Xevo TQD micro mass spectrometer. Chromatographic separation was performed using a CSH analytical column (2.1×100 mm, 1.7μm; Waters) equipped with a guard column (Waters, Milford, MA). Mobile phase A was 7.5mM ammonium bicarbonate pH 7.0, while mobile phase B was 100% methanol. The LC method was 7 minutes, run isocratically at 0.35 mL/minute at 5% mobile phase A and 95% mobile phase B. The following transitions were monitored for M23TC: m/z 841.60→111.99 and m/z 841.60→211.98. Particle size, polydispersity index (PDI), and zeta potential were determined by dynamic light scattering (DLS) using a Malvern Nano-ZS (Worcestershire, UK). Particle morphology was analyzed by transmission electron microscopy (TEM). Samples for TEM imaging were fixed in a solution of 2% glutaraldehyde, 2% paraformaldehyde in 0.1M Sorenson's phosphate buffer (pH 7.2) for a minimum of 24 h at 4°C. Samples were then washed three times with PBS to clear excess fixative. During processing, samples were post-fixed in a 1% aqueous solution of osmium tetroxide for 30 minutes. Subsequently, samples were dehydrated in a graded ethanol series (50, 70, 90, 95, 100%) and propylene oxide was used as a transition solvent between the ethanol and araldite resin. Samples were allowed to sit overnight in a 50:50 propylene oxide:resin solution until all the propylene oxide had evaporated. Samples were then incubated in fresh resin for 2 hours at room temperature before final embedding. Polymerization took place at 65°C for 24 hours. Thin sections (100nm) made with Leica UC6 Ultracut ultramicrotome were placed on 200 mesh copper grids. Sections were stained with 2% Uranyl Acetate followed by Reynolds Lead Citrate, and examined on a Tecnai G^2 Spirit TWIN (FEI) operating at 80kV.

2.3. Half Maximal Effective Concentration (EC_{50}) Measurements

MDMs were cultured in a round bottom 96 well plate (80,000 cells/well) treated with 0.01 nM-10 μM NM23TC or 3TC for 60 min. Medium was replaced with non-drug HIV-1_{ADA} media at a multiplicity of infection (MOI) of 0.1 infectious particles per cell for 4 hours. After 4 hours, infection media was removed, and the cells were incubated an additional 10 days in the presence of the same concentration of drug prior to infection. Half media changes were done every other day. After 10 days of infection, culture media was collected for measures of HIV-1 reverse transcriptase (RT) activity [29–31]. CEM-CD4+ T cells were cultured in suspension in 96 well plates, centrifuged at 650 x *g* and dispersed in 100μL drug-containing media. After 60 minutes, cells were challenged with HIV-$1_{NL4–3\text{-}eGFP}$ (MOI 0.01) by spin-inoculation followed by overnight incubation in drug-containing media. The following day, cells were washed 2x with PBS to remove virus and drug-containing media was replaced. Every 2 days, cells were centrifuged at 650 x *g* and resuspended in fresh drug-containing media. Ten days post HIV-challenge, supernatants were collected for RT activity

measurements. The EC_{50} was calculated using sigmoidal 4-point logarithmic regression from RT activity using GraphPad Prism v7.

2.4. Nanoformulation Preparation

Nanoparticles were prepared by high-pressure homogenization (Avestin EmulsiFlex-C3; Avestin Inc, Ottawa, ON, Canada). M23TC (150.0 mg, 1% w/v) was dispersed in 15 mL of P407 polymer solution containing 0.5% w/v P407 dissolved in PBS (75.00 mg P407). The dispersion was stirred for 16 hours at room temperature followed by homogenization for 1–2 hours at 12,000 psi until a particle size within a range of 200–300 nm was achieved with stable zeta potential. Nanosuspensions were purified by stepwise centrifugations. The suspension was first centrifuged at 150 x *g* for 10 minutes to remove aggregated or sedimented particles. The pellet was discarded, and resultant supernatant centrifuged at 20,000 x *g* for 20 minutes. The pellet was then resuspended in 0.2% (w/v) P407 in PBS. Differential centrifugation produced a stable formulation of slightly larger size (200–250 nm) at a final drug concentration of 150–230 mg/mL.

Direct manufacture was also used for animal studies to demonstrate scalability. An initial drug concentration of 200 mg/mL M23TC was dispersed in FDA-approved injectable excipients Tween 20 and $mPEG_{2000}DSPE$ ((0.2% v/v Tween 20, (30.0 mL) and 0.2% w/v $mPEG_{2000}DSPE$ (30.0 mg) in 15 mL PBS)). After 1–2 days of premixing, the dispersion was homogenized until a desired particle size of 250–300 nm was achieved. The resulting concentration of the direct synthesis formulation was stable for up to one month. *In vitro* and bench testing with both excipients showed similar shape, encapsulation, and nanoparticle behavior in cells for uptake, retention, release, and antiretroviral activity in cells (data not shown).

2.4.1. Cell Uptake and Retention—MDM were cultured in 12 well plates and treated with media containing 100 μM NM23TC or 3TC [7, 8]. At 2, 4, and 8 hours post treatment, media was removed, adherent MDM washed twice with PBS and scraped into 1 mL PBS. Cells were counted using an Invitrogen Countess Automated Cell Counter (Carlsbad, CA) and pelleted by centrifugation at 3,000 x *g*. The cell pellet was reconstituted in 200 μl methanol, sonicated and then centrifuged at 20,000 x *g* for 20 min. The supernatant was analyzed for drug content using LC/MS-MS using a Waters TQD system as described above. Transmission electron microscopy (TEM) was used to image the morphology of MDM.

2.4.2 Triphosphate (3TC-TP) Measurements—For drug retention measures, the cells were incubated with 100 μM drug for 8 h. Drug containing media was removed and cells washed twice with PBS and replaced in media without drug, followed by half media changes every other day until collection. At days 1–30, cells were washed twice with PBS to remove extracellular drug, collected and intracellular drug quantitated. Drug levels were normalized to the number of live cells. Intracellular 3TC triphosphate was extracted from cells and (3TC-TP) levels quantified according to established protocols [32]. Twelve well plates were coated with poly-L-lysine solution (100 μg/mL in distilled water) for 1–2 hours. Wells were washed twice with 1mL PBS to remove excess PLL. CEM-CD4+ T cells suspended in RPMI media were then seeded at 1 million cells/well and incubated at 37°C

for 30–45 minutes. Cells were centrifuged at 650 x *g* for 5 minutes, the supernatant was discarded and replaced with 100 μM of NM23TC or 3TC treatment media. At 4 and 8 h post treatment media was removed. Cells were washed, collected, counted, and pelleted as described for MDM. Drug levels were measured using LC/MS-MS and normalized to live cells. For 3TC-TP analysis, cells were treated, collected, and counted as described above then stored in 70% MeOH. Intracellular 3TC triphosphate levels were then measured as described previously [32].

2.4.3. Measures of Antiretroviral Activity—To assess long-term antiretroviral efficacy, MDM were treated with 100 μM NM23TC or 3TC for 8 h. After treatment, cells were washed with PBS and cultured with fresh media without drug followed by half-media exchanges every other day. At days 1, 5, 10, 15, 20, or 30 after treatment, cells were challenged with HIV-1_{ADA} at a MOI of 0.1 for 16 hours. HIV-1_{ADA} media was then replaced with fresh media without virus. Ten days after viral challenge culture media was analyzed for RT activity, while adherent MDM were fixed with 4% paraformaldehyde and HIV-1 p24 protein expression assessed by immunocytochemistry [29, 33, 34].

2.5. NM23TC Pharmacokinetics (PK) and Drug Biodistribution (BD)

Sprague Dawley rats (Jackson Labs, Bar Harbor, ME, USA) were administered a single 75 mg/kg 3TC-equivalent dose of 3TC or NM23TC intramuscularly (IM) into the caudal thigh muscle to determine PK over 4 weeks. Whole blood and tissue samples were analyzed by LC-MS/MS to determine parent and prodrug levels. Briefly, 25μL blood collected in 1mL acetonitrile and stored at −80°C for later analysis. Liver, spleen, and lymph nodes were collected and sectioned for drug or 3TC-TP analysis. Tissue was homogenized in a solution of 90% methanol/10% water. 100 μL of tissue homogenate was then added to 1mL of ice-cold methanol. For blood and tissue analysis, the acetonitrile or methanol precipitated blood and tissue were vortexed 3 minutes, followed by 10-minute centrifugation at 16000 x *g*. The resulting supernatant was aspirated into a new tube and dried down via vacuum. Samples were reconstituted in 80% methanol M23TC was quantitated via UPLC-MS/MS. 3TC-TP levels were measured in lymph nodes and spleen by LC/MS-MS according to previously published protocols [32]. Toxicity assessment was also conducted in Sprague Dawley rats for 14 days following single IM NM23TC injection at 45 mg/kg 3TC-equivalent dose of 3TC. White blood cells quantification and serum chemistry analysis were performed at day 1, 3, 7 and 14 following NM23TC administration. White blood cells were quantitated using a VetScan HM5 (Abaxis Veterinary Diagnostics, Union City, CA, USA) and serum chemistry analysis was done using a VetScan VS-2 instrument (Abaxis Veterinary Diagnostics, Union City, CA, USA).

2.6. Statistics

Laboratory cell-based studies were performed in triplicate and presented as mean ± standard deviation. Animal groups contained 5 animals per group (n = 5), with one exception in the NM23TC group of animals (n=3). No outliers from animal or cell experiments were excluded. Differences were considered significant at a P-value of <0.05. All the data were analyzed using GraphPad Prism 7.0 software (La Jolla, CA). For pharmacokinetic parameter calculations, Phoenix WinNonlin 8.0 software was used.

2.7. Study Approvals

All animal studies were approved by the University of Nebraska Medical Center Institutional Animal Care and Use Committee in accordance with the standards incorporated in the Guide for the Care and Use of Laboratory Animals (National Research Council of the National Academies, 2011).

3. Results

3.1. M23TC Synthesis and Characterizations

A 3TC ProTide was synthesized by coupling an aryl phenylalanyl docosyl ester phosphorochloridate to the native drug in the presence of ^{t}BuMgCl [21] to form M23TC with a yield of 65% after purification (Fig. 1A). The chemical structure was characterized by ^{1}H-NMR, ^{13}C-NMR, and ^{31}P-NMR. The broad singlet at 0.85 ppm and multiplets at 1.14–1.33 ppm correspond to the terminal methyl and methylene protons of the docosyl ester, respectively. Chemical shifts at 7.10–7.35 ppm represent the aryl and phenylalanine masking promoieties (Fig. 1B). Analyses of ^{13}C-NMR (Supplemental Fig. 1A) and ^{31}P-NMR (Supplemental Fig. 1B) spectra confirmed the successful M23TC synthesis. Doubling of peaks in the carbon, proton and phosphorous spectra demonstrate formation of two isomers at the phosphorous atom. Further chemical characterization of M23TC by FTIR showed absorption bands at 2845 cm^{-1} and 2852 cm^1 corresponding to asymmetric and symmetric C-H stretches from the long chain fatty alcohol (Supplemental Fig. 1C, D). Infusion into a Waters Xevo TQ-S micro mass spectrometer confirmed a molecular mass ion of 841.54, which corresponds to M23TC (Supplemental Fig. 1E).

3.2. Physicochemical Characteristics of M23TC

M23TC showed > 1000-fold reduced aqueous solubility compared to native 3TC. This result confirmed the expected hydrophobicity produced from the lipid conjugate. The solubility of M23TC in 1-octanol was 130 mg/mL and confirming a substantial increase in prodrug lipophilicity (Supplemental Fig. 1F). Based upon water solubility calculations, we then measured the stability of M23TC in PBS and plasma from multiple mammalian species. M23TC was stable in PBS (data not shown) while plasma incubation resulted in prodrug degradation of < 30% over 24 h (Supplemental Fig. 1G). To further evaluate potential biological changes of the modified 3TC, we determined mitochondrial activity by MTT (MDM) and cell viability (CEM-CD4$^+$ T cells). No adverse effects on mitochondrial activity or cell viability were observed at 200 and 50 μM in MDM (Fig. 2A) and CEM-CD4+ T cells, respectively (Fig. 2B). Reflective of M23TC's lipophilicity and poor aqueous solubility, efficacy studies were performed with homogeneous prodrug nanosuspensions (NM23TC). The EC_{50} of NM23TC was decreased 3-fold compared to 3TC (6.2 nM and 19.4 nM, respectively; P=.6121) in MDM (Fig. 2C). EC_{50} analysis of NM23TC in CEM-CD4+ T cells showed a 2-fold decrease in potency compared to native 3TC (79.7nM and 35.4 nM, Fig. 2D). TEM images showed the intracellular presence of nanoformulations after short-term treatment (Fig. 2 E, F, G, H).

3.3. Characterization of NM23TC

We generated P407 M23TC nanoformulations (NM23TC) by high-pressure homogenization. Drug encapsulation efficiency of the synthesized NM23TC nanocrystals was 72%. The size, polydispersity index (PDI), and zeta potential of NM23TC nanocrystals were 189.5 ± 6.1 nm, 0.26 ± 0.01, and −21 ± 0.2 mV, respectively, and remained stable at 25°C for at least 30 days (Fig. 3A). We evaluated NM23TC nanoparticle morphologies by transmission electron microscopy (TEM) (Fig. 3B). NM23TC exhibited uniform spherical particle shape of 151–201 nanometer diameter. Particle stability, uniformity, zeta potential, and EC_{50} measurements supported the formulation integrity.

3.4. Nanoparticle-Cell Interactions

To characterize HIV-nanoparticle interactions, we evaluated cellular uptake and conversion of M23TC to 3TC-TP in MDM and CEM CD4+ T cells. These were measured with single exposure to equivalent concentrations for all compounds and formulations followed by drug and 3TC-TP analyses. NM23TC was readily taken up by MDM with an intracellular drug concentration increasing to 48 μg/10^6 MDM at 24 h (Fig. 3C) more than 50 times higher than that seen for native drug (< 0.5 μg/10^6 cells over 24 h). NM23TC conversion to active metabolite reached a maximum at 8 h with 3TC-TP levels of 16,798 fmol/10^6 cells, significantly greater than that observed with 3TC treatment (4,747 fmol/10^6 cells) (Fig. 3D). Uptake studies in CEM CD4+ T cells showed rapid prodrug uptake (18.3 μg/mL) and conversion of prodrug to 3TC-TP (4067 fmoles/million cells) after 8 hours (Fig. 3E, F). As predicted by the EC_{50} assays, conversion of 3TC to 3TC-TP in CEM CD4+ T cells was rapid. Taken together, these findings demonstrate substantial conversion to 3TC-TP in both HIV-1 target cells (MDM and CD4+ T cells).

Prior data from our laboratories demonstrate long-term storage capacities for nanoformulations in MDM [35, 36]. Thus, retention of NM23TC in MDM was determined. NM23TC facilitated retention of drug in cells for up to 30 days (14 μg/10^6 cells), while native 3TC treatments showed no detectable drug within 24 hours (Fig. 4A). Intracellular active metabolite 3TC-TP was retained by MDM at levels of 3,088 fmol/10^6 cells at day 1 then fell below the limit of quantitation by day 10 following native 3TC treatments. However, NM23TC provided sustained 3TC-TP concentrations of 9,874 and 839 fmol/10^6 cells at days 1 and 30, respectively (Fig. 4B). Media collected from retention studies showed that M23TC was released from at 1685 ng/mL at day 1, and 229.6 ng/mL at day 30 (Fig. 4C).

3.5. Antiretroviral Activities

To assess whether enhanced intracellular 3TC-TP levels from NM23TC would translate into improved antiretroviral activities, MDM were treated with NM23TC or 3TC for 8 hours, followed by drug washout and HIV-1_{ADA} challenge at days 1 through 30. In cells treated with NM23TC, 6.1% breakthrough was seen at day 20, with 16% breakthrough at day 30 (Fig. 4 D, E). In contrast, viral breakthrough was observed within one day following treatment with native 3TC. Cross validation by HIV-1p24 antigen staining paralleled RT results, demonstrating substantial inhibition in virus production for up to 30 days after a single exposure to NM23TC in MDM. A decrease in NM23TC concentration resulted in

increased RT activity (Fig. 4F). These findings demonstrate that NM23TC improves intracellular delivery of 3TC-TP with enhanced drug potency and sustained antiretroviral efficacy.

3.6. Toxicology, PK and BD

NM23TC formulation was manufactured using safe excipients and clinically relevant prodrug lipid linkages. We evaluated NM23TC formulations for toxicity over 2 weeks in Sprague-Dawley rats by measuring serum chemistry and white blood cell counts (Supplementary Fig. 2A). Comparisons were made between NM23TC and control untreated animals. No adverse events were observed in NM23TC treated animals (Supplemental Fig. 2 B, C, D, E **and our unpublished observations)**. For PK and BD studies, male Sprague Dawley rats were administered 75 mg/kg 3TC equivalents of NM23TC (n=3) or 3TC via intramuscular injection. Mice were bled at 2 hours, 1 day, 7 days, 14 days, 21 days, and sacrificed on day 28. A single administration of NM23TC provided sustained and high prodrug concentrations in blood at one month (Fig. 5A). At days 1 and 28, prodrug concentrations in blood were 711 and 103 ng/mL, respectively. In contrast, 3TC provided high native drug concentrations in blood at day 1 which then fell below the limit of quantitation by day 7 (data not shown). Of importance, at day 28 liver (495 ng/g), lymph nodes (4,471 ng/g), and spleen (2,787 ng/g) exhibited high M23TC concentrations (Fig. 5 B, C and D) with detectable levels of 3TC-TP in lymph nodes and spleen (Fig. 5 C and D). As expected, native drug treatment provided drug levels at or below the limits of quantitation (0.05 ng/mL) in plasma and tissues after one day (data not shown). The high M23TC levels in tissues compared to drug concentrations in blood suggest that tissues, especially spleen and lymph nodes, could serve as drug depots for sustained release of M3TC and 3TC-TP. Pharmacokinetics analysis indicated a 17.8 day mean residence time for drug over a 28 day period in blood (Supplemental Fig. 3). Substantial improvements in potency and longer duration of intracellular action of NM23TC could potentially enable reduced dosage and infrequent drug administration.

4. Discussion

A first generation 3TC prodrug produced modest improvements in the drug's half life [11, 20] with limited intracellular drug levels [32]. Thus, we pursued the design and development of a second generation LA 3TC ProTide (M23TC) nanoformulation (NM23TC). The later showed improved drug potency, lipophilicity, stability and antiretroviral activity facilitating enhanced intracellular and tissue drug delivery. In the design of M23TC, phenylalanine was selected based on inherent hydrophobicity and prior studies [22, 37]. The rationale for use of a docosyl ester was based on lipophilicity affecting membrane permeability and inherent antiviral activities, including its synergistic effects on nucleoside analogs [38, 39]. Extensive prior good laboratory practice genotoxicity studies performed in rats, rabbits and dogs supported the prodrug's safety as these modifications failed to demonstrate mutagenic or genotoxic effects after docosanol exposures [40, 41]. In parallel studies, the added lipid content exhibited no untoward effects on reproduction behavior in rats and rabbits [40, 41]. Improvement of 3TC hydrophobicity and lipophilicity, nonetheless, enhanced the

stabilization and conversion of the prodrug into LA ART nanosuspensions also extending the apparent drug half-life.

The development of LA antiretroviral nanomedicines presents attractive alternatives in the prevention and treatment of HIV-1 and for co-morbid infections [32–34] and building on the concept of transforming short acting ARVs into potent tissue targeted nanocrystals with expanded PK and antiretroviral profiles [6]. The potential of LASER ART to improve drug BD and extend ARV half-life are now proven [7, 8, 34, 42]. Indeed, notable advances are highlighted by success of CAB and RPV LA. These were shown to elicit comparable antiretroviral activities to daily oral three-drug regimens during maintenance therapy [4]. However, limitations abound that include rapid ARV metabolism and inherent physicochemical limitations. To overcome such concerns we generated lipophilic LASER ART nanocrystals through chemical modifications of native ART to affect drug potency and ensure rapid transport across physiological barriers [7, 8, 11, 12, 14]. The creation of such formulations served to maximize drug loading with optimization excipient usage while maintaining scalability and storage for potential broad use [15].

We reasoned that drug modifications would be required if a “true” LA formulation was to be obtained for a spectrum of ARVs. Therefore, our laboratory and others explored modification of the primary hydroxyl or amine groups in 3TC to form hydrophobic ester or carbamate prodrug derivatives in attempts to balance the drug’s physiochemical properties and potency. These served to facilitate membrane permeability [11, 20]. However, such strategies only provided limited intracellular drug levels [32]. Notably, prior attempts to use ProTide technology that has proven effective in the discovery of sofosbuvir and tenofovir alafenamide failed to provide enhancement in drug potency when applied to 3TC [43–45]. Thus, we developed alternative strategies that could potentially overcome formulation challenges for short acting ARVs through structure-based screening of a range of amino acid and phosphonate ester promoieties that culminated in identification of a lipophilic sustained release formulation. To this end, a poloxamer coated abacavir (ABC) ProTide nanosuspension (NM3ABC) was made with improved antiretroviral activity [16]. It is worth noting that while the concept of ProTide technology was established a few decades ago [18, 21], its application to NRTIs had focused on improvements of drug potency and safety profile and none have appeared as part of LA regimens. Also, unlike LA formulations of CAB or RPV that have advanced to phase III clinical trials [23, 24], ProTides used in the clinic are characterized by high aqueous solubility, limiting their potential transformation into LA nanosuspensions. Considering the challenges and costs involved in the identification and development of new chemical entities with high potency, acceptable safety profiles as well as ease of formulation into LA therapies, we chose to modify an existing drug into lipophilic ProTide nanocrystals to provide prolonged intracellular accumulation of 3TC-TP while improving drug biodistribution to infection sites and without compromising drug potency. We envisioned that controlled and sustained intracellular delivery of 3TC monophosphate could potentially limit adverse effects by maintaining intracellular active drug levels within the therapeutic range.

Limitations of NRTIs include shorter drug half-lives, variable PK profiles and poor drug penetrance into cellular and tissue reservoirs of infection, thereby increasing the likelihood

of developing drug resistant virus strains [46, 47]. To overcome these hurdles, kinase bypass strategies such as the phosphoramidate ProTide technology have been explored and led to the discovery of potent antiviral agents [18, 19]. However, prior studies in MDMs demonstrated that application of the ProTide strategy to 3TC results in significant reduction in antiretroviral activity of the modified compounds in comparison to the parent drug [48]. In addition, the few reported examples of 3TC monophosphate analogs are either hydrolytically unstable or susceptible to enzymatic dephosphorylation rendering such molecules less efficacious [44, 45]. Therefore, clinical application of conventional ProTide approaches to 3TC required further optimization. We report herein the design and development of a LA 3TC ProTide (M23TC) formulation (NM23TC) with improved drug potency, lipophilicity and stability in plasma for enhanced intracellular and tissue drug delivery.

Development of sustained release aqueous suspension forms of hydrophilic NRTIs is a significant challenge. Our initial attempts to use an ester prodrug approach to formulate NRTIs provided only limited intracellular active TP levels. With these challenges in mind, we combined optimized ProTide and nanocrystal strategies to produce a long acting slow effective release 3TC prodrug formulation referred to as NM23TC. The prodrug formulation demonstrated a three-fold improvement in EC_{50} in human MDM when compared to native 3TC. This is notable since previous studies with phosphoramidate derivates of 3TC in MDM and CEM CD4+ T cells demonstrated diminished potency when compared to native 3TC treatment [48]. The enhanced antiviral activity observed for NM23TC is likely due to either improved cellular drug uptake and activation or potential synergism between 3TC TP and the docosanol masking group [38, 39].

The success of LA HIV-1 formulations is dependent on efficient delivery and sustained release of therapeutic concentrations of drug at cellular and tissue reservoirs of infection. Specifically, sustained intracellular drug concentrations could disrupt the viral replication cycle and prevent further viral dissemination over time. To evaluate intracellular delivery and activation of NM23TC, human MDM and CEM CD4+ T cells were used. Previous work from our laboratory has shown that storage of nanoformulated antiretroviral drugs in endosomal compartments provides protection from drug metabolism [35, 36]. This could explain the delayed release of M23TC from MDM over 30 days. NM23TC significantly enhanced cellular drug uptake and retention compared to native 3TC. To exert antiviral activity, M23TC must undergo intracellular metabolism to form 3TC TP [49]. The mechanism of activation and influence of masking groups on ProTide bioactivation has previously been described [50, 51]. To affirm intracellular activation of M23TC, we quantified 3TC-TP levels in MDM and CEM CD4+ T cells in parallel drug uptake and retention studies. In these studies, NM23TC exhibited enhanced and sustained intracellular drug release profiles with the active metabolite levels detectable for up to 30 days. The 3TC-TP response was measurable at 30 days and concurrently exhibited superior antiretroviral activity compared to native 3TC as measured by HIV RT activity and HIV-1 p24 antigen staining. The slight increase in 3TC-TP at day 30 is attributable to several factors. Though the 3TC-TP measurement assay is well vetted, several intra-assay steps add small degrees for error at each point. 3TC-TP values were normalized to viable cells. Therefore, a slight decrease in cell viability at day 25 and 30 may selectively promote cells with specific

enzymatic machinery. An excess of 3TC-monophosphate or 3TC-diphosphate in early timepoints could further account for increased production of 3TC-TP at later timepoints. Lastly, cell-nanoformulation interactions may affect 3TC-TP levels. Dissolution of the nanocrystal within the cell and long-term nanoformulation stability within MDM may change over time. Because of enhanced 3TC-TP levels, NM23TC exhibited superior antiretroviral activity compared to native 3TC as measured by HIV RT activity and HIV-1 p24 antigen staining. The antiviral activity was sustained for 30 days after single treatment with NM23TC. Of importance, no cytotoxicity was observed at drug concentrations used for cellular studies. These results demonstrate that NM23TC enhances drug potency and sustained intracellular efficacy.

Given that effective treatment and prevention of HIV-1 is dependent on achieving consistent therapeutic ART levels in plasma and tissues [52, 53], we evaluated the PK and tissue distribution profiles of NM23TC in rats. A single intramuscular injection of NM23TC provided sustained and high drug concentrations in blood and tissues over one month. In contrast, drug concentrations from native 3TC treatment fell below the limit of quantitation within a day. High intracellular and tissue drug levels for NM23TC could potentially translate into reduced dosage [17]. Of significance, NM23TC treated animals showed high 3TC-TP levels in lymph nodes and spleen at one month compared to undetectable levels for the native drug treatment suggesting efficient and sustained conversion of M23TC to its active form upon release from nanocrystals. Overall, improvement in lipophilicity, plasma stability and tissue distribution of M23TC has the potential to overcome limitations of the native drug or previously described ProTide approaches. Previous studies have shown that prodrugs that exhibit increased stability in plasma could enhance potency and intracellular accumulation of nucleosides in vivo [18]. These data sets demonstrate that transformation of 3TC from an oral daily dosage into potent LA formulations is achievable.

In summary, a novel long acting slow effective release NM23TC ProTide nanoformulation was developed, exhibiting enhanced intracellular 3TC-TP concentrations that paralleled potent antiretroviral activities for at least 30 days in MDM and improved drug uptake in CD4+ T cells. The high concentrations of drug observed in tissues of animals exposed to NM23TC could potentially translate to improved efficacy and restrict low-level viral replication that occurs in lymphoid tissues during combination antiretroviral therapy treatment. Furthermore, the potency and extended duration of action of NM23TC could promote treatment regimen adherence. Future studies will evaluate the anti-HIV efficacy of NM23TC formulations in animal models of HIV-1 infection.

Supplementary Material

Refer to Web version on PubMed Central for supplementary material.

Acknowledgments

We wish to thank the University of Nebraska Medical Center Cores for Electron Microscopy (Tom Bargar & Nicholas Conoan), NMR Spectroscopy (Ed Ezell), Elutriation and Cell Separation (Myhanh Che and Na Ly). This research was supported by the University of Nebraska Foundation, which includes donations from the Carol Swarts, M.D. Emerging Neuroscience Research Laboratory, the Margaret R. Larson Professorship, and the Frances, and Louie Blumkin, and Harriet Singer Endowment, the Vice Chancellor’s Office of the University of Nebraska

Medical Center for Core Facility Developments, and National Institutes of Health grants R01 MH104147, P01 DA028555, R01 NS36126, P01 NS31492, 2R01 NS034239, P01 MH64570, P30 MH062261, P30 AI078498, R01 AG043540 and 1 R56 AI138613-01A1.

Abbreviations

3TC-lamivudine	2’,3’-Dideoxy-3’-Thiacytidine
3TC-TP	3TC-triphosphate
ABC	abacavir
ART	antiretroviral therapy
ARV	antiretroviral drugs
CAB	cabotegravir
CEM	cellosaurus cell line
DTG	dolutegravir
EC_{50}	half maximal effective concentration
FTC	emtricitabine
FTIR	Fourier transform infrared spectroscopy
HIV-1	human immunodeficiency virus type one
LA	long-acting
LASER ART	long-acting slow release antiretroviral therapy
LC-MS	liquid chromatography-mass spectrometry
LPV	lopinavir
M23TC	3TC ProTide
MDM	monocyte-derived macrophages
NM23TC	nanoformulated 3TC ProTide
NMR	nuclear magnetic resonance
NRTI	nucleoside reverse transcriptase inhibitor
PD	pharmacodynamics
PK	pharmacokinetics
ProTide	prodrug nucleotide
RPV	rilpivirine
RPV LA	rilpivirine long-acting

TAF	tenofovir alafenamide
TEM	transmission electron microscopy

References

[1]. Katz IT, Maughan-Brown B, Improved life expectancy of people living with HIV: who is left behind?, Lancet HIV 4(8) (2017) e324–e326. [PubMed: 28501496]

[2]. Nachega JB, Marconi VC, van Zyl GU, Gardner EM, Preiser W, Hong SY, Mills EJ, Gross R, HIV treatment adherence, drug resistance, virologic failure: evolving concepts, Infect Disord Drug Targets 11(2) (2011) 167–74. [PubMed: 21406048]

[3]. Margolis DA, Boffito M, Long-acting antiviral agents for HIV treatment, Curr Opin HIV AIDS 10(4) (2015) 246–52. [PubMed: 26049949]

[4]. Margolis DA, Gonzalez-Garcia J, Stellbrink HJ, Eron JJ, Yazdanpanah Y, Podzamczer D, Lutz T, Angel JB, Richmond GJ, Clotet B, Gutierrez F, Sloan L, Clair MS, Murray M, Ford SL, Mrus J, Patel P, Crauwels H, Griffith SK, Sutton KC, Dorey D, Smith KY, Williams PE, Spreen WR, Long-acting intramuscular cabotegravir and rilpivirine in adults with HIV-1 infection (LATTE-2): 96-week results of a randomised, open-label, phase 2b, non-inferiority trial, Lancet 390(10101) (2017) 1499–1510. [PubMed: 28750935]

[5]. Barnhart M, Long-Acting HIV Treatment and Prevention: Closer to the Threshold, Glob Health Sci Pract 5(2) (2017) 182–187. [PubMed: 28655797]

[6]. Edagwa B, McMillan J, Sillman B, Gendelman HE, Long-acting slow effective release antiretroviral therapy, Expert opinion on drug delivery (2017) 1–11.

[7]. Sillman B, Bade AN, Dash PK, Bhargavan B, Kocher T, Mathews S, Su H, Kanmogne GD, Poluektova LY, Gorantla S, McMillan J, Gautam N, Alnouti Y, Edagwa B, Gendelman HE, Creation of a long-acting nanoformulated dolutegravir, Nat Commun 9(1) (2018) 443. [PubMed: 29402886]

[8]. Zhou T, Su H, Dash P, Lin Z, Dyavar Shetty BL, Kocher T, Szlachetka A, Lamberty B, Fox HS, Poluektova L, Gorantla S, McMillan J, Gautam N, Mosley RL, Alnouti Y, Edagwa B, Gendelman HE, Creation of a nanoformulated cabotegravir prodrug with improved antiretroviral profiles, Biomaterials 151 (2018) 53–65. [PubMed: 29059541]

[9]. Quercia R, Perno CF, Koteff J, Moore K, McCoig C, St Clair M, Kuritzkes D, Twenty-Five Years of Lamivudine: Current and Future Use for the Treatment of HIV-1 Infection, J Acquir Immune Defic Syndr 78(2) (2018) 125–135. [PubMed: 29474268]

[10]. Cihlar T, Ray AS, Nucleoside and nucleotide HIV reverse transcriptase inhibitors: 25 years after zidovudine, Antiviral Res 85(1) (2010) 39–58. [PubMed: 19887088]

[11]. Guo D, Zhou T, Arainga M, Palandri D, Gautam N, Bronich T, Alnouti Y, McMillan J, Edagwa B, Gendelman HE, Creation of a Long-Acting Nanoformulated 2',3'-Dideoxy-3'-Thiacytidine, J Acquir Immune Defic Syndr 74(3) (2017) e75–e83. [PubMed: 27559685]

[12]. Singh D, McMillan J, Hilaire J, Gautam N, Palandri D, Alnouti Y, Gendelman HE, Edagwa B, Development and characterization of a long-acting nanoformulated abacavir prodrug, Nanomedicine (Lond) 11(15) (2016) 1913–27. [PubMed: 27456759]

[13]. McMillan J, Szlachetka A, Slack L, Sillman B, Lamberty B, Morsey B, Callen S, Gautam N, Alnouti Y, Edagwa B, Gendelman HE, Fox HS, Pharmacokinetics of a Long-Acting Nanoformulated Dolutegravir Prodrug in Rhesus Macaques, Antimicrob Agents Chemother 62(1) (2018).

[14]. McMillan J, Szlachetka A, Zhou T, Morsey B, Lamberty B, Callen S, Gautam N, Alnouti Y, Edagwa B, Gendelman HE, Fox HS, Pharmacokinetic testing of a first generation cabotegravir prodrug in rhesus macaques, AIDS (2018).

[15]. Zhou T, Lin Z, Puligujja P, Palandri D, Hilaire J, Arainga M, Smith N, Gautam N, McMillan J, Alnouti Y, Liu X, Edagwa B, Gendelman HE, Optimizing the preparation and stability of decorated antiretroviral drug nanocrystals, Nanomedicine (Lond) 13(8) (2018) 871–885. [PubMed: 29553879]

[16]. Lin Z, Gautam N, Alnouti Y, McMillan J, Bade AN, Gendelman HE, Edagwa B, ProTide generated long-acting abacavir nanoformulations, Chem Commun (Camb) 54(60) (2018) 8371–8374. [PubMed: 29995046]

[17]. Ray AS, Fordyce MW, Hitchcock MJ, Tenofovir alafenamide: A novel prodrug of tenofovir for the treatment of Human Immunodeficiency Virus, Antiviral Res 125 (2016) 63–70. [PubMed: 26640223]

[18]. Mehellou Y, Rattan HS, Balzarini J, The ProTide Prodrug Technology: From the Concept to the Clinic, J Med Chem (2017).

[19]. Ray AS, Hostetler KY, Application of kinase bypass strategies to nucleoside antivirals, Antiviral Res 92(2) (2011) 277–91. [PubMed: 21878354]

[20]. Agarwal HK, Chhikara BS, Hanley MJ, Ye G, Doncel GF, Parang K, Synthesis and biological evaluation of fatty acyl ester derivatives of (−)-2',3'-dideoxy-3'-thiacytidine, J Med Chem 55(10) (2012) 4861–71. [PubMed: 22533850]

[21]. Cahard D, McGuigan C, Balzarini J, Aryloxy phosphoramidate triesters as pro-tides, Mini Rev Med Chem 4(4) (2004) 371–81. [PubMed: 15134540]

[22]. McGuigan C, Harris SA, Daluge SM, Gudmundsson KS, McLean EW, Burnette TC, Marr H, Hazen R, Condreay LD, Johnson L, De Clercq E, Balzarini J, Application of phosphoramidate pronucleotide technology to abacavir leads to a significant enhancement of antiviral potency, J Med Chem 48(10) (2005) 3504–15. [PubMed: 15887959]

[23]. Williams PE, Crauwels HM, Basstanie ED, Formulation and pharmacology of long-acting rilpivirine, Curr Opin HIV AIDS 10(4) (2015) 233–8. [PubMed: 26049947]

[24]. Trezza C, Ford SL, Spreen W, Pan R, Piscitelli S, Formulation and pharmacology of long-acting cabotegravir, Curr Opin HIV AIDS 10(4) (2015) 239–45. [PubMed: 26049948]

[25]. Landovitz RJ, Kofron R, McCauley M, The promise and pitfalls of long-acting injectable agents for HIV prevention, Curr Opin HIV AIDS 11(1) (2016) 122–8. [PubMed: 26633643]

[26]. Callebaut C, Stepan G, Tian Y, Miller MD, In Vitro Virology Profile of Tenofovir Alafenamide, a Novel Oral Prodrug of Tenofovir with Improved Antiviral Activity Compared to That of Tenofovir Disoproxil Fumarate, Antimicrob Agents Chemother 59(10) (2015) 5909–16. [PubMed: 26149992]

[27]. Noell BC, Besur SV, deLemos AS, Changing the face of hepatitis C management - the design and development of sofosbuvir, Drug Des Devel Ther 9 (2015) 2367–74.

[28]. Gendelman HE, Orenstein JM, Martin MA, Ferrua C, Mitra R, Phipps T, Wahl LA, Lane HC, Fauci AS, Burke DS, et al., Efficient isolation and propagation of human immunodeficiency virus on recombinant colony-stimulating factor 1-treated monocytes, J Exp Med 167(4) (1988) 1428–41. [PubMed: 3258626]

[29]. Balkundi S, Nowacek AS, Veerubhotla RS, Chen H, Martinez-Skinner A, Roy U, Mosley RL, Kanmogne G, Liu X, Kabanov AV, Bronich T, McMillan J, Gendelman HE, Comparative manufacture and cell-based delivery of antiretroviral nanoformulations, International journal of nanomedicine 6 (2011) 3393–404. [PubMed: 22267924]

[30]. Kalter DC, Nakamura M, Turpin JA, Baca LM, Hoover DL, Dieffenbach C, Ralph P, Gendelman HE, Meltzer MS, Enhanced HIV replication in macrophage colony-stimulating factor-treated monocytes, J Immunol 146(1) (1991) 298–306. [PubMed: 1701795]

[31]. Nowacek AS, McMillan J, Miller R, Anderson A, Rabinow B, Gendelman HE, Nanoformulated antiretroviral drug combinations extend drug release and antiretroviral responses in HIV-1-infected macrophages: implications for neuroAIDS therapeutics, J Neuroimmune Pharmacol 5(4) (2010) 592–601. [PubMed: 20237859]

[32]. Gautam N, Lin Z, Banoub MG, Smith NA, Maayah A, McMillan J, Gendelman HE, Alnouti Y, Simultaneous quantification of intracellular lamivudine and abacavir triphosphate metabolites by LC-MS/MS, J Pharm Biomed Anal 153 (2018) 248–259. [PubMed: 29518644]

[33]. Nowacek AS, Balkundi S, McMillan J, Roy U, Martinez-Skinner A, Mosley RL, Kanmogne G, Kabanov AV, Bronich T, Gendelman HE, Analyses of nanoformulated antiretroviral drug charge, size, shape and content for uptake, drug release and antiviral activities in human monocyte-derived macrophages, J Control Release 150(2) (2011) 204–11. [PubMed: 21108978]

[34]. Puligujja P, Balkundi SS, Kendrick LM, Baldridge HM, Hilaire JR, Bade AN, Dash PK, Zhang G, Poluektova LY, Gorantla S, Liu XM, Ying T, Feng Y, Wang Y, Dimitrov DS, McMillan JM, Gendelman HE, Pharmacodynamics of long-acting folic acid-receptor targeted ritonavir-boosted atazanavir nanoformulations, Biomaterials 41 (2015) 141–50. [PubMed: 25522973]

[35]. Arainga M, Guo D, Wiederin J, Ciborowski P, McMillan J, Gendelman HE, Opposing regulation of endolysosomal pathways by long-acting nanoformulated antiretroviral therapy and HIV-1 in human macrophages, Retrovirology 12 (2015) 5. [PubMed: 25608975]

[36]. Gnanadhas DP, Dash PK, Sillman B, Bade AN, Lin Z, Palandri DL, Gautam N, Alnouti Y, Gelbard HA, McMillan J, Mosley RL, Edagwa B, Gendelman HE, Gorantla S, Autophagy facilitates macrophage depots of sustained-release nanoformulated antiretroviral drugs, J Clin Invest 127(3) (2017) 857–873. [PubMed: 28134625]

[37]. McGuigan C, Devine KG, O'Connor TJ, Kinchington D, Synthesis and anti-HIV activity of some haloalkyl phosphoramidate derivatives of 3'-azido-3'-deoxythymidine (AZT): potent activity of the trichloroethyl methoxyalaninyl compound, Antiviral Res 15(3) (1991) 255–63. [PubMed: 1888176]

[38]. Marcelletti JF, Synergistic inhibition of herpesvirus replication by docosanol and antiviral nucleoside analogs, Antiviral Res 56(2) (2002) 153–66. [PubMed: 12367721]

[39]. Katz DH, Marcelletti JF, Pope LE, Khalil MH, Katz LR, McFadden R, n-docosanol: broad spectrum anti-viral activity against lipid-enveloped viruses, Ann N Y Acad Sci 724 (1994) 472–88. [PubMed: 8030975]

[40]. Iglesias G, Hlywka J, Berg JE, Khalil MH, Pope LE, Tamarkin D, The toxicity of behenyl alcohol. I. Genotoxicity and subchronic toxicity in rats and dogs, Regul Toxicol Pharmacol 36(1) (2002) 69–79. [PubMed: 12383719]

[41]. Iglesias G, Hlywka JJ, Berg JE, Khalil MH, Pope LE, Tamarkin D, The toxicity of behenyl alcohol. II. Reproduction studies in rats and rabbits, Regul Toxicol Pharmacol 36(1) (2002) 80–5. [PubMed: 12383720]

[42]. Gautam N, Puligujja P, Balkundi S, Thakare R, Liu XM, Fox HS, McMillan J, Gendelman HE, Alnouti Y, Pharmacokinetics, biodistribution, and toxicity of folic acid-coated antiretroviral nanoformulations, Antimicrob Agents Chemother 58(12) (2014) 7510–9. [PubMed: 25288084]

[43]. Balzarini J, Wedgwood O, Kruining J, Pelemans H, Heijtink R, De Clercq E, McGuigan C, Anti-HIV and anti-HBV activity and resistance profile of 2',3'-dideoxy-3'-thiacytidine (3TC) and its arylphosphoramidate derivative CF 1109, Biochem Biophys Res Commun 225(2) (1996) 363–9. [PubMed: 8753770]

[44]. Jessen HJ, Schulz T, Balzarini J, Meier C, Bioreversible protection of nucleoside diphosphates, Angew Chem Int Ed Engl 47(45) (2008) 8719–22. [PubMed: 18833560]

[45]. Wagner CR, Iyer VV, McIntee EJ, Pronucleotides: toward the in vivo delivery of antiviral and anticancer nucleotides, Med Res Rev 20(6) (2000) 417–51. [PubMed: 11058891]

[46]. Grossman Z, Polis M, Feinberg MB, Grossman Z, Levi I, Jankelevich S, Yarchoan R, Boon J, de Wolf F, Lange JM, Goudsmit J, Dimitrov DS, Paul WE, Ongoing HIV dissemination during HAART, Nat Med 5(10) (1999) 1099–104. [PubMed: 10502799]

[47]. Furtado MR, Callaway DS, Phair JP, Kunstman KJ, Stanton JL, Macken CA, Perelson AS, Wolinsky SM, Persistence of HIV-1 transcription in peripheral-blood mononuclear cells in patients receiving potent antiretroviral therapy, N Engl J Med 340(21) (1999) 1614–22. [PubMed: 10341273]

[48]. Aquaro S, Wedgwood O, Yarnold C, Cahard D, Pathinara R, McGuigan C, Calio R, de Clercq E, Balzarini J, Perno CF, Activities of masked 2',3'-dideoxynucleoside monophosphate derivatives against human immunodeficiency virus in resting macrophages, Antimicrob Agents Chemother 44(1) (2000) 173–7. [PubMed: 10602742]

[49]. Balzarini J, Herdewijn P, De Clercq E, Differential patterns of intracellular metabolism of 2',3'-didehydro-2',3'-dideoxythymidine and 3'-azido-2',3'-dideoxythymidine, two potent anti-human immunodeficiency virus compounds, J Biol Chem 264(11) (1989) 6127–33. [PubMed: 2539371]

[50]. Birkus G, Kutty N, He GX, Mulato A, Lee W, McDermott M, Cihlar T, Activation of 9-[(R)-2-[[(S)-[[(S)-1-(Isopropoxycarbonyl)ethyl]amino] phenoxyphosphinyl]-methoxy]propyl]adenine

(GS-7340) and other tenofovir phosphonoamidate prodrugs by human proteases, Mol Pharmacol 74(1) (2008) 92–100. [PubMed: 18430788]

[51]. Birkus G, Wang R, Liu X, Kutty N, MacArthur H, Cihlar T, Gibbs C, Swaminathan S, Lee W, McDermott M, Cathepsin A is the major hydrolase catalyzing the intracellular hydrolysis of the antiretroviral nucleotide phosphonoamidate prodrugs GS-7340 and GS-9131, Antimicrob Agents Chemother 51(2) (2007) 543–50. [PubMed: 17145787]

[52]. Pantaleo G, Graziosi C, Demarest JF, Butini L, Montroni M, Fox CH, Orenstein JM, Kotler DP, Fauci AS, HIV infection is active and progressive in lymphoid tissue during the clinically latent stage of disease [see comments], Nature 362(6418) (1993) 355–8. [PubMed: 8455722]

[53]. Embretson J, Zupancic M, Ribas JL, Burke A, Racz P, Tenner-Racz K, Haase AT, Massive covert infection of helper T lymphocytes and macrophages by HIV during the incubation period of AIDS [see comments], Nature 362(6418) (1993) 359–62. [PubMed: 8096068]

Highlights

1. Synthesis of a hydrophobic 3TC ProTide (M23TC) and subsequent formulation (NM23TC)
2. NM23TC enhanced drug uptake in multiple HIV-1 relevant cell lines, rapidly converting to 3TC-TP
3. M23TC was released from monocyte-derived macrophages (MDM) over 30 days after single administration.
4. NM23TC exerted substantial antiretroviral activity in MDM over 30 day $HIV\text{-}1_{ADA}$ challenge
5. A single intramuscular injection of 75 mg/kg (3TC eq.) in rats produced detectable 3TC-TP in spleen and lymph nodes for 28 days

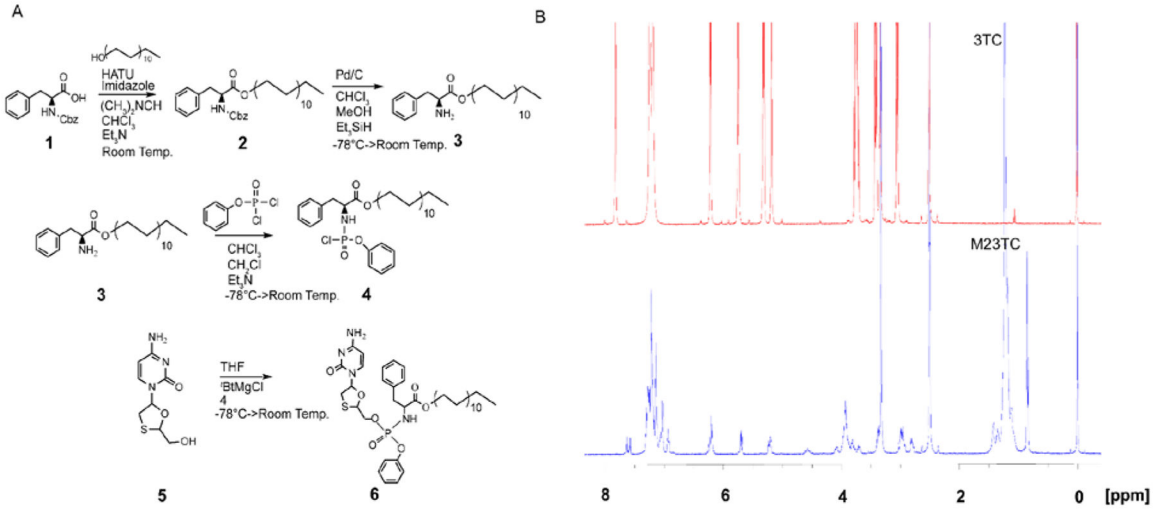

Figure 1. Synthesis and characterization of M23TC.

(A) Synthesis of aryl amino phosphochloridate masking group as previously described [16]. Briefly, Cbz protected phenylalanine (**1)** was reacted with docosanol to give (**2)**, followed by Cbz cleavage to yield **3**. Benzyl dichlorophosphonate was then reacted with **3** to give the aryl amino phosphochloridate masking group (**4**). The masking group was conjugated to 3TC **(5)** using ^{t}BuMgCl base in anhydrous THF to form M23TC in 65% yield **(6)**. **(B)** Proton NMR spectra of 3TC (in red) and M23TC (in blue): ^{1}H-NMR (M23TC), (500 MHz, (CD3)2S=O): 7.88 (d, J = 7.3 Hz 1H), 7.60 (app. d, J = 7.6 Hz 1H), 7.10–7.35 (m, 8 H), 7.03 (app. d, J = 7.9 Hz 2H), 6.15–6.29 (m, 1H), 5.65–5.75 (m, 1H), 5.19–5.29 (m, 1H), 3.92 (br, 5H), 3.35–3.48 (m, 4H), 2.90–3.02 (m, 1H), 2.75–2.85 (m, 1H), 1.42 (br, 2H), 1.14–1.33 (m, 38H), 0.85 (br, 3H)

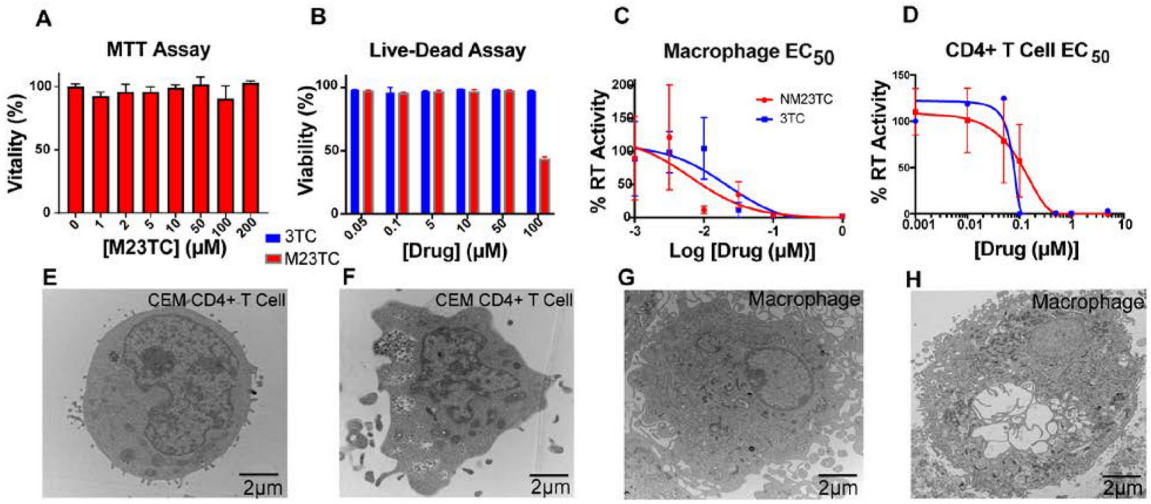

Figure 2. Physicochemical and biological characterization of M23TC and NM23TC.

(A) MTT assay of MDM 24 h after M23TC treatment over a concentration range of 1–200μM. Results were normalized to untreated control MDM. M23TC was found to be nontoxic up to 200 μM. Data are represented as mean +/− SEM for n=3 samples per group. **(B)** CEM CD4+ T cell vitality using LiveDead Staining. CEM CD4+ T cells plated in a 96 well plate at 100,000 cells/well were treated with a ranged of 3TC or M23TC concentrations from 0.05–100μM. Data are represented as mean +/− SEM for n=3 samples per group. **(C)** EC_{50} was determined in MDM by measuring RT activity in the supernatant for 3TC and NM3TC over a concentration range of 1nM-1μM (EC_{50}=6.2 nM for NM23TC, 19.4 nM for 3TC). **(D)** EC_{50} was measured in CD4+ T cells over a concentration range of 1nM-10μM by measuring RT activity of supernatant and normalized to % of positive control (EC_{50}=79.7 nM for NM23TC, 35.4 nM for 3TC). **(E-H)** TEM morphological evaluation in MDM and CEM-CD4+ T CD4+ T cells. Cells were treated with 100μM NM23TC for 8 hours. Control cells (E and G) were given no treatment and collected alongside treated cells (F and H).

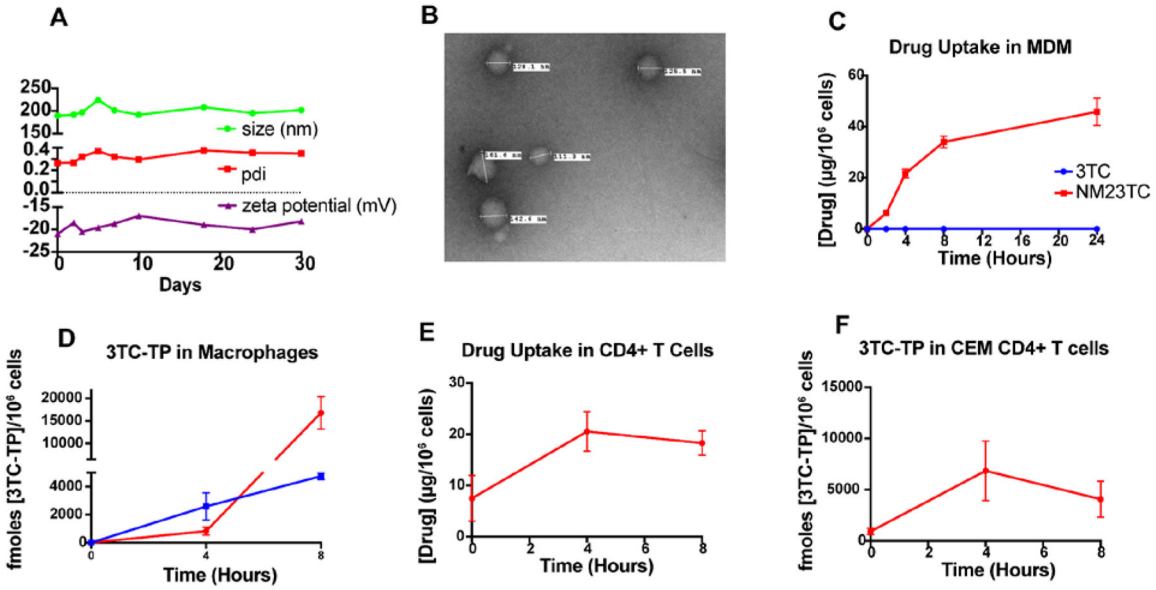

Figure 3. M23TC nanoformulation (NM23TC) characterization and cell-nanoparticle interactions:

(A) M23TC was stabilized by a solution of P407 in PBS via high-pressure homogenization to form nanosuspensions (NM23TC) that were characterized by size, PDI, and zeta potential**. (B)** TEM images of NM23TC. MDMs treated for 24 hours with 100 μM NM23TC or 3TC measured as **(C)** drug (shown in red for NM23TC and blue for 3TC) and conversion to **(D)** 3TC-TP. CEM-CD4+ T CD4+ cells treated for 8 h with 10 μM NM23TC and **(E)** drug and **(F)** 3TC-TP levels were determined.

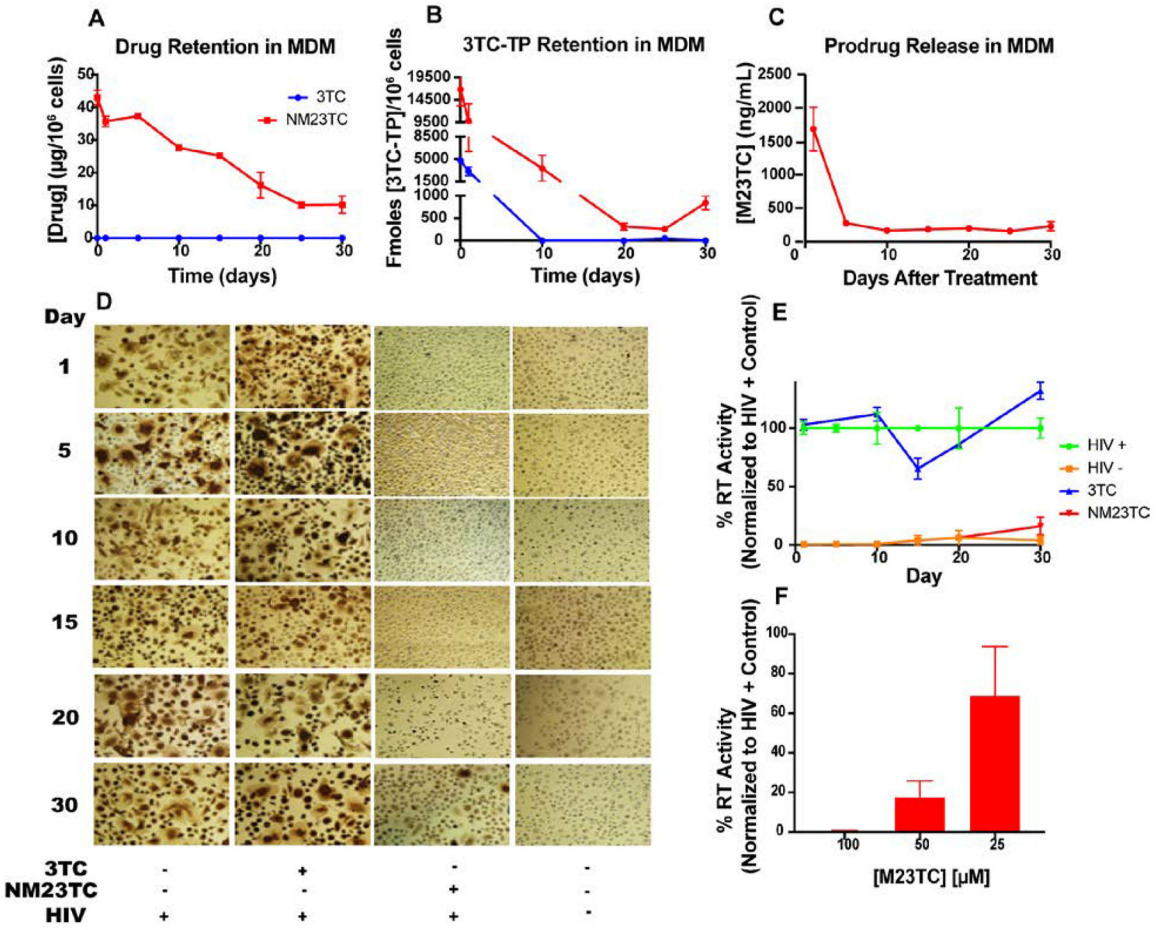

Figure 4. NM23TC long-term cell-nanoparticle interactions and efficacy:

M23TC levels after a single 8 h media treatment of 100 μM NM23TC or 3TC, followed by PBS wash and replacement with fresh medium over 30 days. **(A)** Drug and **(B)** 3TC-TP were quantified at days 1, 5, 10, 15, 20, 25, and 30 after treatment removal. **(C)** Release of prodrug from MDM into culture medium at days 1, 5, 10, 15, 20, 25, and 30 after treatment removal. Long-term antiretroviral efficacy was determined. At days 0, 1, 5,10, 15, 20, and 30 after an 8 h drug loading with 100μM 3TC or NM3TC, MDM were challenged with HIV-1_{ADA} at 0.1 MOI for 4 h. Untreated infected and untreated uninfected cells served as positive and negative controls, respectively. Viral media was replaced with fresh media and cells were cultured for an additional 10 days. Medium was collected for HIV reverse transcriptase (RT) activity measurement; **(D)** corresponding cells were fixed in paraformaldehyde and stained for HIV-1 p24 antigen (brown)**. (E)** HIV RT activities were measured and expressed as a percentage of RT activities in HIV-1 infected untreated MDM. **(F)** RT activities in cells pre-treated with 100, 50, or 25 μM NM23TC and infected 10-days later with HIV-1_{ADA}.

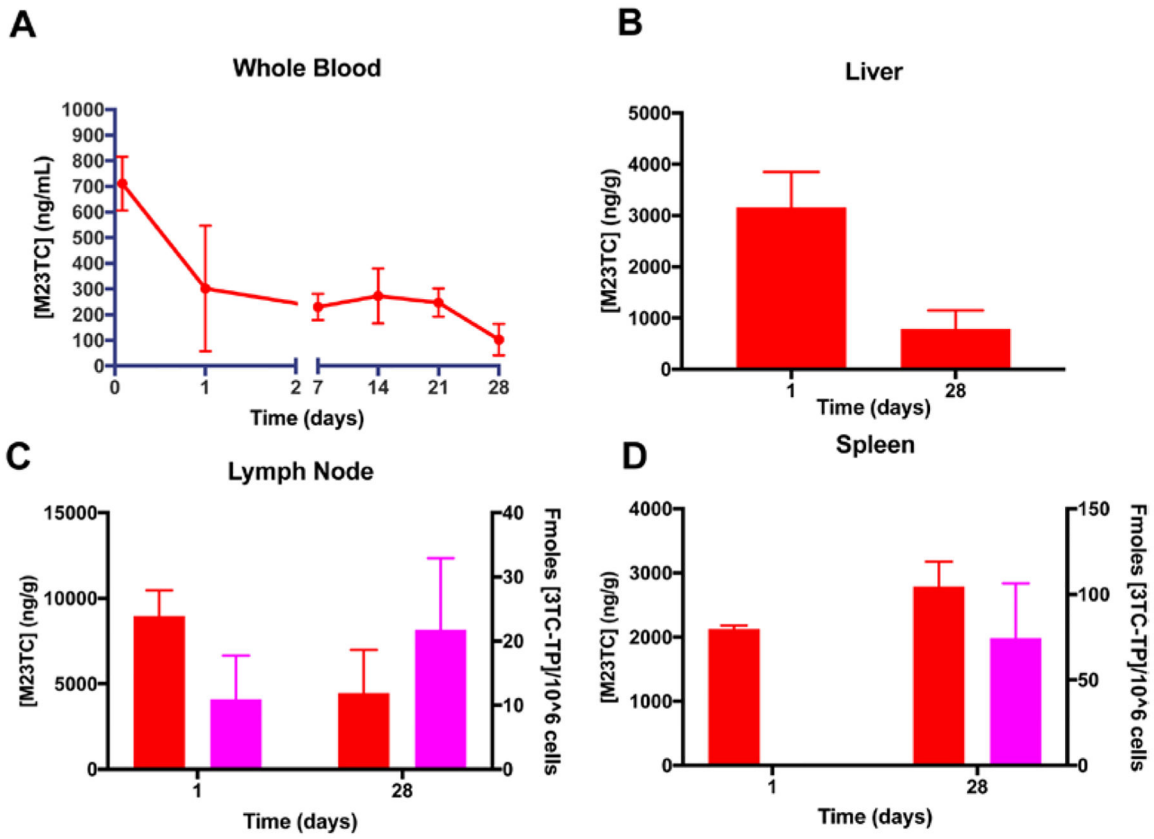

Figure 5. NM23TC pharmacokinetics:

Sprague-Dawley rats were given a single IM injection of 75 mg/kg 3TC equivalents as NM23TC. **(A)** Prodrug concentrations in whole blood were measured at days 1,7,14, 21, and 28**. (B)** Prodrug levels in liver were measured at days 1 and 28. Prodrug (red) and 3TC-TP (magenta) levels in **(C)** lymph node, and **(D)** spleen were determined at days 1 and 28.